Materials Today Sustainability 34 (2026) 101344

Contents lists available at ScienceDirect

Materials Today Sustainability

journal homepage: www.journals.elsevier.com/materials-today-sustainability

Material characterisation of bioplastics: Influence of different starch sources in fish gelatin-based blends

Jade Stanley [a,1], Clément Poulain [b,1], Frédéric Debeaufort [b,c,*], Claire-Hélène Brachais [d], David Culliton [e], Nasreddine Benbettaieb [b,c], Antonio-Jonay Jovani-Sancho [f], Adriana Cunha Neves [a]

[a] Department of Applied Science, South East Technological University Carlow, Kilkenny Rd, Moanacurragh, Carlow, R93 V960, Ireland
[b] Université Bourgogne Europe, Institut Agro, INRAE, UMR PAM, Dijon, F-21000, France
[c] Université Bourgogne Europe, Institut of Technology – BioEngineering dpt, Dijon, F-21000, France
[d] Université Bourgogne Europe, Laboratoire Interdisciplinaire Carnot de Bourgogne (ICB), UMR 6303 CNRS, Dijon, France
[e] Department of Aerospace, Mechanical and Electronic Engineering, South East Technological University, Carlow, Kilkenny Rd, Moanacurragh, Carlow, R93 V960, Ireland
[f] United Kingdom Centre for Ecology and Hydrology, Bangor, LL57 2UW, United Kingdom

ARTICLE INFO

Keywords:
Starch-gelatine blend
Bioplastics
Thermal treatment
Structure
Mass transfers
Surface energy

ABSTRACT

The growing environmental concerns regarding petroleum-based plastics have accelerated research into sustainable, alternative materials such as bioplastics or biopolymers. Gelatin-starch blend bioplastics (SPBBs) have gained momentum in research as a possible solution due to their biodegradability, biobased resource and potential for many applications. However, the structural and functional properties of SPBBs, such as barrier performance and rigidity properties, depend on the starch source and the formulation method. This study focuses on characterising SPBBs from potato, tapioca, sago and swamp taro. The aim was to assess the influence of starch composition, evaluated by amylose and amylopectin % ratio, with a specific interest in the relationship between chemical composition and functional properties of the materials. Methods including Fourier Transform Infrared Spectroscopy (FTIR), X-ray Diffraction (XRD), goniometry, water vapour permeability (WVP), oxygen permeability, and Dynamic Mechanical Analysis (DMTA) were used to evaluate the biopolymer's structural integrity, composition and barrier properties. The results revealed no significant variation in amylose to amylopectin ratios and subtle differences in starch profiles; however, once incorporated with the other materials, homogenised profiles were seen. XRD analysis showed distinct polymorphic structures in the raw starches. However, the incorporation of gelatine disrupted the starch structures and inhibited the gelatine's triple helix reconstitution. Surface Free Energy (SFE) analysis showed that potato SPBB demonstrated wettable potential; in contrast, lower SFE and critical surface tension (CST) values of sago SPBB indicated more hydrophobic surfaces, which is ideal for food packaging. The assessed barrier properties showed that SPBBs have good water barrier properties but poor oxygen permeabilities. DMTA results indicated that tapioca SPBB had the highest rigidity, while sago SPBB had properties more suitable for shock-absorbing material applications. Further research is needed to enhance the specific properties of these polymers for particular applications.

1. Introduction

The global demand for plastics has significantly increased plastic pollution, creating extensive environmental repercussions for marine, terrestrial and human health [1]. The rising concerns over plastic pollution, ecosystem damage, and human health have highlighted the urgent need for sustainable alternatives to conventional plastics [2]. Bioplastics have gained interest over recent years to combat plastic

* Corresponding author. Université Bourgogne Europe, Institut Agro, INRAE, UMR PAM, F-21000, Dijon, France.
E-mail addresses: Jade.Stanley@setu.ie (J. Stanley), Clement.Poulain@ube.fr (C. Poulain), frederic.debeaufort@ube.fr (F. Debeaufort), Claire-Helene.Brachais@ube.fr (C.-H. Brachais), David.Culliton@setu.ie (D. Culliton), Nasreddine.Benbettaieb@ube.fr (N. Benbettaieb), jsancho@ceh.ac.uk (A.-J. Jovani-Sancho), Adriana.CunhaNeves@setu.ie (A.C. Neves).
[1] These two authors contributed equally to this work.

https://doi.org/10.1016/j.mtsust.2026.101344
Received 9 July 2025; Received in revised form 8 January 2026; Accepted 7 March 2026
Available online 9 March 2026

waste concerns, as bioplastics are primarily produced from bio sources such as agricultural crops and waste streams, indicating excellent biodegradability properties [3]. These biopolymers offer a means to mitigate plastic pollution by providing an environmentally friendly alternative. One promising type of bioplastics is starch-protein blend bioplastics (SPBBs), derived from fish gelatine and starches such as potato, tapioca, sago and swamp taro. These materials are naturally occurring; some come from waste streams and are biodegradable and abundant [4].

In recent years, the application of bioplastics in various industries, packaging, agriculture and consumer goods has gained significant momentum due to their lower environmental impact than traditional plastics [5]. According to European bioplastic [6] definitions, a plastic substance is bioplastic if it is either bio-based, biodegradable, or possesses both qualities. The term "bio-based" denotes that a product, such as starches and proteins, is partially derived from renewable biomass like plants. Bio-based does not automatically imply biodegradable. The ability of a material to degrade through biodegradation is not dependent on its resource basis but rather on how chemically complex it is. Consequently, 100% of bio-based polymers may not biodegrade depending on the treatment used to make them a biopolymer, such as polyamide 11 (PA 11), which is formulated from castor oil [7]. Only when the environment and time are specified does the term "biodegradability" become apparent. The key advantage of SPBBs is their biodegradability, which allows them to disintegrate naturally over time, reducing the environmental footprint. However, their mechanical strength, barrier properties, and water resistance performance remain significant challenges for widespread adoption in packaging industries [8]. To address these issues, starch bioplastics are combined with proteins or other additives to enhance the mechanical and barrier properties [9]. Most studies focus on potato starch-based bioplastics; however, SPBBs made from alternative starches could have unique properties in these polymers [10]. Exploration of this gap in the literature by characterising SPBBs from these alternatives, ideally sustainable, starch sources will provide vital insights for further development of versatile biopolymeric materials for a diverse variety of applications [11,12]. This study focuses on developing and characterising SPBBs from different starch sources – potato, tapioca, sago and swamp taro associated into fish gelatin as the main component of the SPBBS. The objectives are to assess the functional properties of these gelatine-starch blends, including chemical composition, biopolymer polymorphism, surface and barrier properties.

2. Materials and methods

2.1. Materials

Potato starch (M.P. Biomedicals LLC, Amsterdam, The Netherlands), tapioca, sago and swamp taro starches (provided by Dr. Jonay Jovani-Sancho), a food-grade fish gelatine powder, used as a film-forming agent, were purchased from Louis Francois (Marne-La-Vallée, France). The degree of bloom of gelatine is 200, and its viscosity is 3.5–4.5 mPa s at a concentration of 6.6% in water and 60 °C, according to the supplier, which was used to generate bioplastics. Glycerol (EMPROVE®bio, Merck KGaA, Darmstadt, Germany) was used as a plasticiser. Amylose/Amylopectin Assay Kit was purchased from Megazyme (Megazyme, Ireland). Chemicals used for amylose/amylopectin concentration: DMSO from Riedel-de-Haen (Honeywell, Seelze, Germany), anhydrous sodium acetate (Analab, Antrim, UK) and 95% (v/v) ethanol (BDH laboratory, Loughborough, UK). The Whatman® No. 1 filter paper was from Macherey-Nagel, and the permeability cells with aperture Duran lids were from VWR. Chemicals for WVP and goniometry analysis: magnesium chloride, potassium chloride, glycerol and ethylene glycol (min 99% purity, Sigma Aldrich, St Quentin Fallavier, France).

2.2. Making bioplastics

The bioplastics were created using Stanley et al. [3] method using potato, tapioca, sago and swamp taro. Firstly, 10 g of fish gelatine was allowed to bloom in 80 ml of water and then heated until obtaining a clear suspension (about 90 °C) as quick as possible using a hotplate set up to 300 °C. Meanwhile, a slurry was prepared by mixing 5 g of desired starch, 7.5 ml glycerol, and 20 ml of water and then added into the gelatine solution. This accounts for a dry matter ratio of 44.5 % gelatine, 22.2 % starch, and 33.3 % glycerol. Once the mixture was homogenous, after 40 min, it was poured into the desired mould, silicone, and a blowtorch was run over the surface to pop any unwanted bubbles.

2.3. Amylose and amylopectin

The method for completing this procedure strictly followed the kit amylose/amylopectin assay kit, purchased from Megazyme (Scotland, United Kingdom), and samples were read via a Shimadzu UV-1800 UV-vis spectrometer (serial no A11634970166, USA, MFG INC.).

The following calculation using Equation (1) was used to obtain the amylose % content:

$$Amylose, \%\ (w/w) = \frac{\text{Absorbance (Con A Supernatant)}}{\text{Absorbance (Total Starch Aliquot)}} \times \frac{6.15}{9.2} \times 100 \quad \text{Equation 1}$$

Where 6.15 and 9.2 are dilution factors for the Con A and Total Starch extracts, respectively.

2.4. FTIR-ATR

Thermofisher Scientific Fourier transform infrared (FTIR) model: Nicolet is10 (Wisconsin, USA) was used as the instrument equipped with an Attenuated Total Reflection accessory (ATR). The nature of the ATR crystal was a diamond; the parameters were 32 scans, the wavenumber range was 4000-400 cm^{-1}, and a resolution of 4 cm^{-1}. Analyses were conducted both for liquid samples (glycerol) and solid samples – potato, tapioca, sago, swamp taro, fish gelatine and the overall polymer film matrix – using a worm screw for perfect contact between the diamond and the sample surface to determine functional groups.

2.5. XRD

X-ray diffraction was carried out on a Bruker D2 phase, with the instrument equipped with a divergence slit and diffracted beam scatter slit, and the measurement time was 1 h. Prior analysis by XRD, all samples have been equilibrated at 50% RH and 25 °C, same conditions as measurements. The samples were examined over the angular range of 0° to 40° with a step size of 0.024° and a count time of 1.3 s per point for a high resolution. Samples were cut to 4 cm in diameter for the bioplastics; raw samples or the starches and gelatine, both dry and hydrolysed, were also measured. Pre-treatment of the signal was completed by normalisation of the signal, followed by sequential Fourier transformation in order to filter the halo corresponding to both the amorphous parts of the polymer and diffusion of X-ray within the signal. After selection and intensity correction of the background, both the background and subtracted signals were saved.

2.6. Goniometry

The contact angle and surface energy of the SPBB films were measured using a Kruss goniometer (DSA30, Kruss GmbH, Villebon, France) by the sessile drop method [13,14] with various liquids: water, glycerol, ethylene glycol, water-ethylene glycol and water-glycerol (1:1 mass ratios) [15]. Binary liquid mixtures, including water-glycerol and water-ethylene glycol, were used to obtain a range of data points for

determining best-fit parameters in the Owens-Wendt model [15]. Roughly 4 μL of each test liquid was automatically placed on the air-dried side of the films, with measurements taken over 3 min using a camera and Kruss-Advance software (version 2). These measurements included the contact angle (θ), droplet surface area, and volume (V) as functions of time (t). Experiments were conducted in a controlled environment at 25 ± 2 °C and 50 ± 1% relative humidity, with all samples preconditioned to these conditions for at least 3 days prior to the experiment. Each film formulation was tested with at least five replicates.

Surface free energy (γ_S) and critical surface tension (of liquids able to wet the film surface) (γ_C) were assessed using the Laplace–Young approximation and Zisman method, respectively. The critical surface tension was determined by extrapolating the linear regression of cos θ versus the surface tension of various liquids to cos θ = 1 [16]. The liquids used for surface tension measurements were the same as those for the contact angle and surface free energy. Measurements were repeated at least five times for each film formulation. The surface free energy (γ_S), also known as in the case of liquids, along with its dispersive (γ_S^D) and polar (γ_S^P) components were determined using the Owens–Wendt method [17], as demonstrated in Equations (2) and (3) from Ref. [14]:

$$\gamma S = \gamma_S^P + \gamma_S^D \quad \text{Equation 2}$$

$$\gamma_L = (1 + cos\,\Theta) = 2\left(\sqrt{\gamma_L^P \gamma_S^D} + \sqrt{\gamma_L^P \gamma_S^D}\right) \quad \text{Equation 3}$$

Where γ_L is the surface tension of the liquid, γ_L^D and γ_L^P are the dispersive and polar components of the liquid's surface tension, respectively. γ_S^D and γ_S^P are the solid's surface free energy dispersive and polar components, respectively. θ is the contact angle between the baseline of the drop and the tangent at the drop boundary, and the droplet volume.

The surface behaviour of the SPBB's was examined via goniometry to assess their spreading, swelling and absorption abilities, Fig. 1. For wettability measurements, the droplet volume was maintained at a constant level, and a progressive decrease in the contact angle was observed over time, indicating increased surface wetting. In swelling scenarios, the droplet volume would increase as the material absorbed the liquid and expanded below or a part of the solid dissolves in the droplet. This led to variable contact angle trends, where the angle would either increase or decrease over time due to surface wetting. For absorption behaviour, a constant decline in droplet volume over time corresponds to liquid uptake by the polymers. In these cases, the contact angle would either remain constant or reduce, further supporting surface wetting and tend to correspond with swelling behaviour.

2.7. Water vapour permeability and O_2 permeability

Prior all permeability experiments (water vapour and oxygen), all film samples have been equilibrated at 50% RH and at 25 °C.

Water Vapour Permeability (WVP) and Oxygen Permeability (OP) were determined using standardised gravimetric and manometric methods. For the WVP assessment, the gravimetric cup method described in ISO 2528 (2017) and adapted to hydrophilic biopolymers by Debeaufort et al. [18] was employed [19]. Film thickness was determined as the average of five measurements for each formulation. To obtain an internal relative humidity (RH) of 84% inside the permeation cells, film samples were placed between two rubber rings on top of glass cells containing potassium chloride saturated salt solution. Magnesium chloride saturated salt solution was placed in a beaker to yield an external humidity of 33%. Furthermore, these permeation cells were kept at 25 °C in a climate-controlled, ventilated chamber. For every SPBB, measurements were made in four duplicates. The following formula was utilised to determine the water vapour permeability:

$$WVP = \frac{\Delta\, m \times e}{A \times \Delta t \times \Delta p} \quad \text{Equation. 4}$$

Where $\Delta m/\Delta t$ is the weight of moisture loss per unit of time (g s^{-1}), A is the film area exposed to moisture transfer (8.04 × 10^{-4} m^2), e is the film thickness (m), and Δp is the water vapour pressure difference between two sides of the film (Pa).

Oxygen permeability (OP) was measured using Brügger equipment (Type GTT; Brügger Feinmechanik GmBH, Munich, Germany) in accordance with the standard manometric method ISO: 15.105 [20]. A humidified oxygen flow swept the upper side of the permeation cell's test chambers, 50% RH, at a flow rate of roughly 80 mL/min at atmospheric pressure. Both chambers have been degassed under vacuum before oxygen sweeping. An external computer measured and displayed the pressure rise in the downward chamber during the test period. GTT software was used to record data and calculate permeance, and triplicate samples were used. The film thickness was measured after OP determination using an automatic digital calliper to calculate the permeability of each formulation (to prevent any potential cracks due to the probe of the calliper).

2.8. DMTA (Dynamic mechanical thermal analysis)

DMTA was conducted using a DMTA Q800 (TA Instruments, Guyancourt, France) equipped with a calibrated tensile kit with 1.5 cm × 2 mm x 150 μm sample sizes used to determine the glass transition temperatures, loss and storage modulus in a broad temperature range. Using this technique, the moduli of the polymer samples were monitored against the frequency at 1 Hz. The conditions of the measurements were initially to cool at – 80 °C and allowed to stabilise for 5 min. The sample was then gradually heated from – 80 °C to 90 °C at an increased rate of 5 °C/minute. Glass transitions were detected using the tan delta, which is the ratio between the two moduli. All samples have been conditioned at 50% RH and 25 °C prior measurements and equipment located in an air-conditioned room under same conditions.

2.9. Statistical analysis

Shapiro-Wilks tests for normality, one-way analysis of variance (ANOVA) was employed for statistical analysis, and Tukey-Kramer or Kruskal-Wallis analysis was applied as required for all data, dependent on normality testing. P ≤ 0.05 was the significance threshold, with statistically significant differences indicated by different script letters: A, B, C and so forth. Excel (Excel 2021, version 2108) and SPSS Statistics (IBM SPSS Statistics 28.0.0 version, 2020) were utilised as the analysis software.

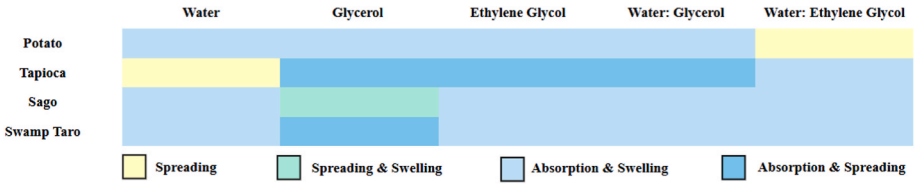

Fig. 1. Heatmap of kinetic surface behaviour of the biopolymers with various solvents used.

3. Results and discussion

3.1. Amylose and amylopectin

The amylose and amylopectin ratios from Fig. 2 showed that potato, tapioca, sago and swamp taro results for each starch type corroborate what is presented in the literature with tapioca's amylose content ranging from as low as 17 % to 26.1 % [21,22], sago's from 20.61 % to 37 % [23,24] and swamp taro from 14.1 % to 30.62% [25,26]. This wide range is due to multiple factors such as variety, location and, in the case of Taro, its corm size [27]. Literature reports similar amylose content (between 26.3 and 30.7%) in potato starch when tested with the same method used in this work [28]. The amylose and Amylopectin content (%) of starches– potato, tapioca, sago and swamp taro – displayed no statistical difference (values of Fig. 2 represent the mean of N = 3 for each sample, ±standard deviation using a value of P > 0.05, ANOVA and Tukey Kramer).

3.2. FTIR

The FTIR-ATR was used to compare the different starches' chemical structure and identify specific interactions between the various components of the SPBB formulations and displayed in Fig. 3. FTIR spectra of starch powder: potato, tapioca, sago and swamp taro, focused the interesting and functional groups- 3280-3290 cm^{-1} (O-H stretching), 2880-2930 cm^{-1} (C-H stretching), 1450-1410 cm^{-1} (CH2 bending), 1335 cm^{-1} (OH bending), 900-1150 cm^{-1} (C-O-C, C-O-H stretching and bending).

As starches are a mixture of amylose and amylopectin - two glucose polymers - the typical bands for those polyether-polyol materials (Fig. 3) appear at 3280-3290 cm^{-1} (broad band, O-H stretching), 2880-2930 cm^{-1} (doublet, C-H stretching), 1450-1410 cm^{-1} (CH_2 bending), 1335 cm^{-1} (OH bending in the plane), 900-1150 cm^{-1} (C-O-C, C-O-H stretching and bending), which was consistent with the literature [12,29]. Indeed, a supplementary absorbance is noted at 1550 cm^{-1}, which can be assigned to C-N bending. A much higher intensity for the 1635 cm^{-1} band can refer to a carbonyl stretching band overlaying the band accounting for OH bending due to water absorption [12,29], a common characteristic in hydrophilic polymers [30]. These two last bands can be the signature of residual proteins in the swamp taro powder. All the starches displayed strong transmittance near 1000 cm^{-1}, corresponding to C-O stretching vibrations common to starches, confirming a similar glucose-based backbone [31,32]. Literature from Ref. [33] on potato bioplastics and [34] on tapioca polymers produced similar results, except the 1050 cm^{-1} was lower down; this could have been due to the bioplastic composition. While small spectral shifts existed within the SPBBs, the overall ATR-FTIR profiles remained very similar between starch sources.

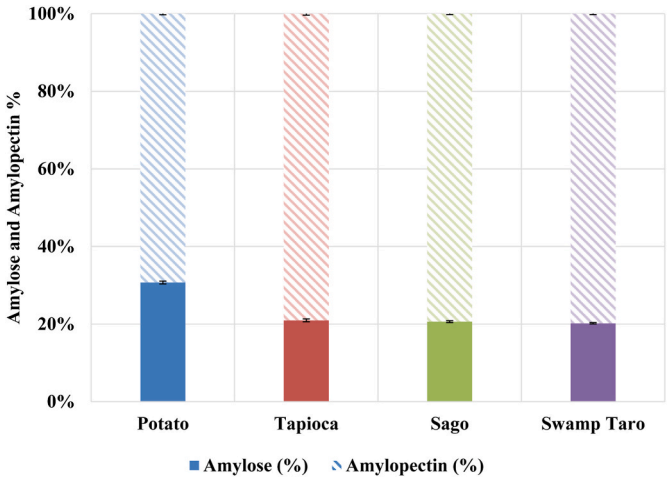

Fig. 2. Amylose and amylopectin content (%) of starches– potato, tapioca, sago and swamp taro.

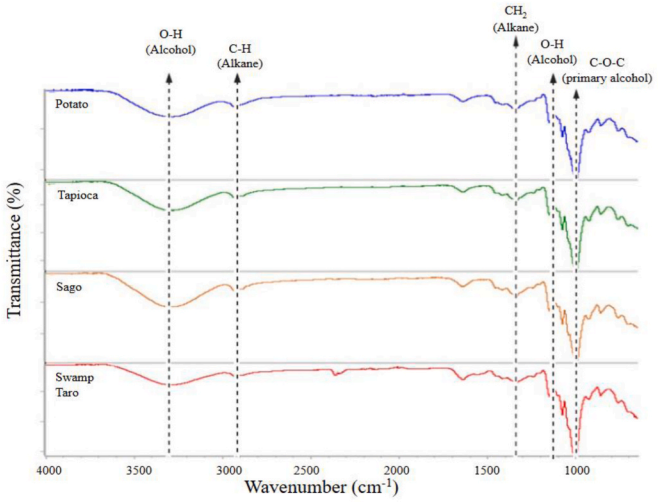

Fig. 3. FTIR spectra of starch powder: potato, tapioca, sago and swamp taro.

To assist in interpreting the final bioplastic spectra (Fig. 6), the FTIR profiles of glycerol and fish gelatine were also examined and presented in Figs. 4 and 5, respectively. Fish gelatine showed a broad O–H and N–H stretching vibration band, also visible in the 3200–3400 cm^{-1} region, reflecting hydrogen bonding potential [35]. Characteristic amide peaks, including Amide I (1650 cm^{-1}), which indicates C=O peptide bonds; Amide II (1540 cm^{-1}) and Amide III (1240 cm^{-1}), demonstrating N-H bending, all indicators of protein structures [36]. These amide peaks are particularly important in the context of the bioplastic blend, as they suggest that gelatine contributes a distinct set of polar functional groups capable of interacting with both the hydroxyl groups of the starch and the polyol groups of the glycerol (Pérez-Marroquín et al., 2022). Moreover, the proteinaceous nature of gelatine introduces a more amorphous component to the blend, which may disrupt the crystallinity of the starch component, thus enhancing the ductility of the bioplastic (Pérez-Marroquín et al., 2022; [32]). This synergistic behaviour has been reported in several studies involving starch-protein blends, where the protein acts as a structural modifier [12,33].

Glycerol demonstrated a very broad O–H stretching band around 3300 cm^{-1}, followed by a -CH stretching at 2800-2900 cm^{-1}, Fig. 5, overlapping with starch and bioplastic spectra. There were wide bands in the 1300-1000 cm^{-1} region indicating groups of C-O symmetric and asymmetric stretching, alongside a sharp peak in the 1000 cm^{-1} region

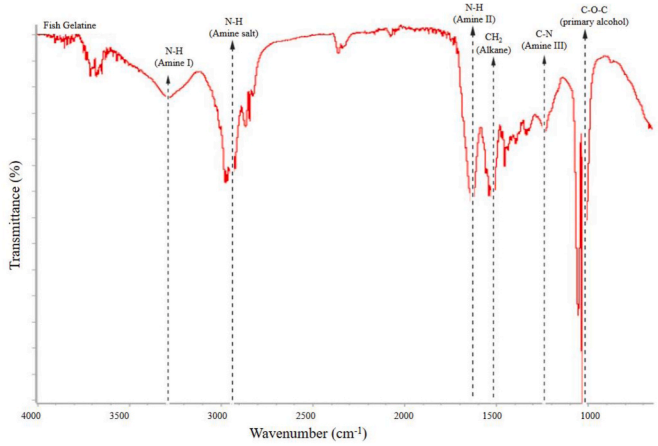

Fig. 4. FTIR spectra of neat fish gelatine granules.

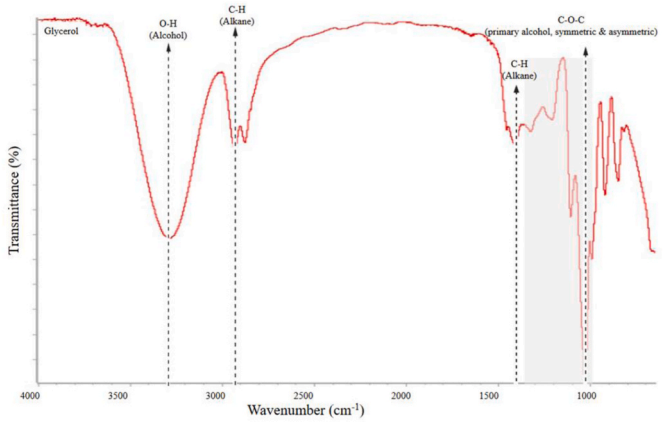

Fig. 5. FTIR spectra of the glycerol liquid.

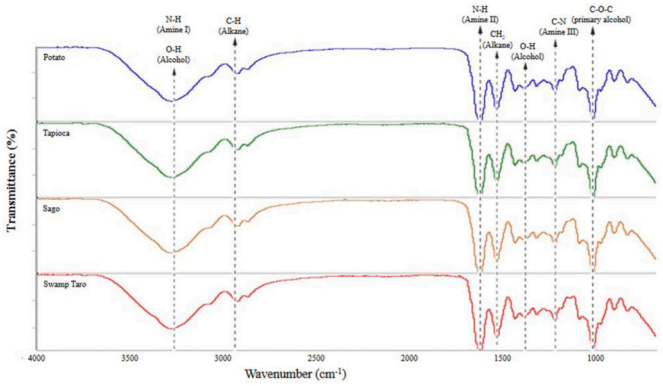

Fig. 6. FTIR spectra of the biopolymer blend materials.

associated with an asymmetric C–O, as expected [37]. Consequently, the presence of glycerol influenced the polymer network by contributing to the homogeneous spectral profiles observed in the SPBBs across all polymer types, as shown in Fig. 6.

The O-H groups initially exhibited different intensities, as shown in Fig. 3; however, as biopolymers, Fig. 6, these bands now overlap, likely due to hydrogen bonding interactions with the O-H groups of glycerol, Fig. 5. The broad bands at the 3300 cm^{-1} regions, indicating O-H, indicate intermolecular bonding in the material, aligning with this. The transmittance at 2900 cm^{-1} and 1600 cm^{-1} increases in intensity, suggesting further interaction involving glycerol and fish gelatine, as shown in Figs. 4 and 5. The region between 1400 and 1200 cm^{-1} revealed distinctive stretching, potentially arising from overlapping vibrational modes of the added plasticiser and protein. Where the bioplastic components interacted, all Figs. 3–6 showed a C-O stretching band near 1000 cm^{-1}, characteristic of polysaccharide and alcohol structures [38,39].

The data was shown in Fig. 3D displayed strong, broad bands at 3300 cm^{-1} (O–H stretching), consistent with forming a hydrogen-bonded network. A medium C–H stretch was present at 2910 cm^{-1}, and a pronounced band at 1640 cm^{-1} displayed the carbonyl glucose from starch, corresponding to findings from Ref. [12,29]. The alcohol and ether C-O bond can be seen in the medium peak at 1350 cm^{-1} and an intense stretch at 1000 cm^{-1}, respectively (Neves et al., 2020; [29]). These bands confirm the presence of polysaccharide structures and support the overlapping chemical compositions of the different starches. Although the starches might have slightly different structures, their chemical composition is similar. Another 1620 - 1650 cm^{-1} peak corresponds to water absorption [40]. For the bioplastics created, there was an O-H strong, broad stretch at 3295 cm^{-1}, a medium C-H stretch was found at 2910 cm^{-1}, the region of 1630 cm^{-1} showed an intense C=C stretch, the cluster at 1450-1400 cm^{-1} that indicated a medium O-H bond, at 1040 cm^{-1} a strong C-O stretch.

It could be concluded that the origin of starch and the addition of gelatine did not majorly modify the chemical bonds and altered the interactions within the starch networks of the films. The FTIR results confirm the homogenous blending of starch and gelatine and support the compatibility of both components in the SPBB matrices. It should be noted that ATR-FTIR is not the most sensitive technique for identifying subtle structural differences between similar polysaccharides, such as differentiating between amylose and amylopectin [32], a limitation also highlighted by Warren et al. [41] in their ATR-FTIR analysis of starch polymorphs. Therefore, despite small shifts or intensity changes, no significant differences could be conclusively identified across starch sources or their corresponding SPBBs.

3.3. XRD

Fig. 7 showed the XRD diffractograms associated with the raw starches of potato (A), tapioca (B), sago (C) and swamp taro (D). The blue signal represents the raw data from the instrument, the red signal represents the halo, and the yellow signal represents the treated signal. The vertical blue and red dotted lines correspond to the polymorphic type of the samples, B and A type, respectively, with the vertical green dotted line (around 2 θ theta = 20°) indicating the V-type region.

The results of the XRD on the raw starches are depicted in Fig. 7, allowing to identify their polymorphic structures based on the positions and relative intensities of the reflections of A and B-type structures. This was determined from the atomic plane coordinates found by Talja et al. [42], Lopez-Rubio et al. [43] and Mutungi et al. [44]. Potato starch displayed a typical B-polymorph (Fig. 7A) while tapioca starch exhibited the A-polymorph (Fig. 7B). Both sago (Fig. 7C) and swamp taro (Fig. 7D) starches appeared to contain a mixture of the signature doublets of A and B types, with peaks at 17.1° and 18.1°for the A type and a strong peak at 5.5° for the B type [44]; these were classified as C-polymorphs.

Generally, cereal starches belong to the A-polymorph, whereas tuber and amylose-rich starches belong to B-polymorph, and legumes and some tuber starches are categorised as C-polymorph [44]. A- and B-polymorphs arise from left-handed parallel double-helical strands assembled in monoclinic and hexagonal lattice symmetries respectively. A higher density of packing of double helices and fewer water molecules in the A-polymorph interstices than the B-polymorph is the main structural difference between the two polymorphs [44]. The C-polymorph is formed when both A- and B-polymorphic arrangements co-exist. Another crystalline arrangement, the V-form, is also categorised but is based on single-helical glucopyranosyl chains [44]. V-polymorph is identified by a reflection at 19.8° (Mutungi et al., 2012) and is a denatured starch type due to swelling retrogradation. These crystalline forms also appear when gelatinised starch re-crystallises under different conditions [44].

With the addition of other plasticisers, such as glycerol, the structure of starch can be altered, as discussed in the literature. Starch is a semi-crystalline biopolymer containing both crystalline and amorphous phases contributed by amylose, a linear structure, and amylopectin, a branched structure [45,46]. During film formation, the crystalline peaks of the starch molecules are transformed into semi-crystalline or amorphous patterns due to granular disruption, and the dissociated starch chains interact with glycerol to form a V-polymorph. During the films' drying, the recrystallisation of amylose and amylopectin can result in the starch films' semi-crystalline structure [46]. Piyawatakarn et al. [47] identified similar findings suggesting that glycerol should affect the formation of different crystalline forms, which might also affect other properties of the films.

Other plasticisers, such as water combined with glycerol, have been noted to change the structure of starch molecules. When the gelatinisation of starch with water is completed, it destroys the crystalline starch

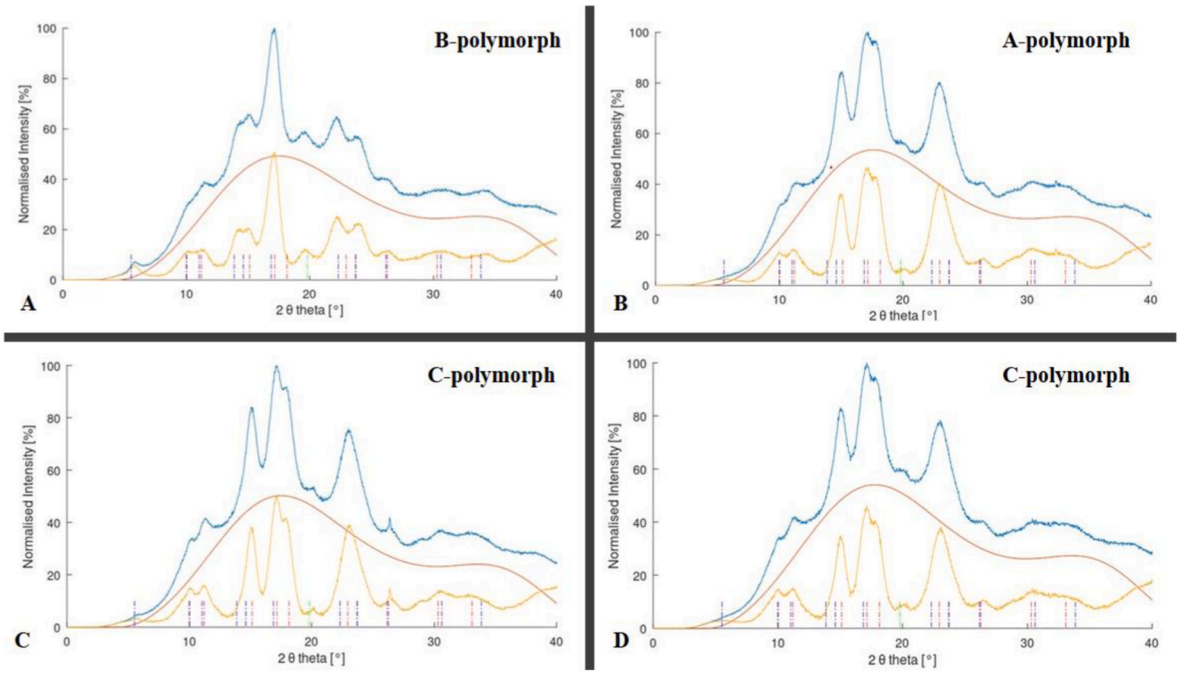

Fig. 7. A – D XRD diffractograms associated with the raw starches of potato (A), tapioca (B), sago (C) and swamp taro (D). The blue signal represents the raw data from the instrument, the red signal represents the halo, and the yellow signal represents the treated signal.

structure and, as a result, changes the crystalline nature. Bidardi et al., 2023 and [45] found the nature of such films to be amorphous with soft characteristics, ideal for food packaging.

Water is often used when creating starch-protein-based films. Therefore, it is crucial to understand how it affects starch molecules. Fig. 8 gives the XRD diffractograms of potato, tapioca, sago and swamp taro starches hydrolysed by water (again the blue signal represents the raw data from the instrument, the red signal represents the halo, and the yellow signal represents the treated signal; the blue and red dotted lines correspond to the polymorphic type of the samples, B and A type, respectively, with the green dotted line indicating the V-type region). Fig. 8 showed how the peaks in the images became sharper when water was introduced to the starches, gelatinising them. How gelatinisation works regarding starch is through water absorption into the granules, leading to hydration of the amorphous shell and disrupting the hydrogen bonds, leading to the irreversible destruction of molecular order within the granules [48]. Therefore, the sharpening of the peaks in the XRD images could be attributed to the mobility of starch molecules that is favoured by moisture and then could easily recrystallise.

The addition of fish gelatine to the starch-protein blend bioplastics

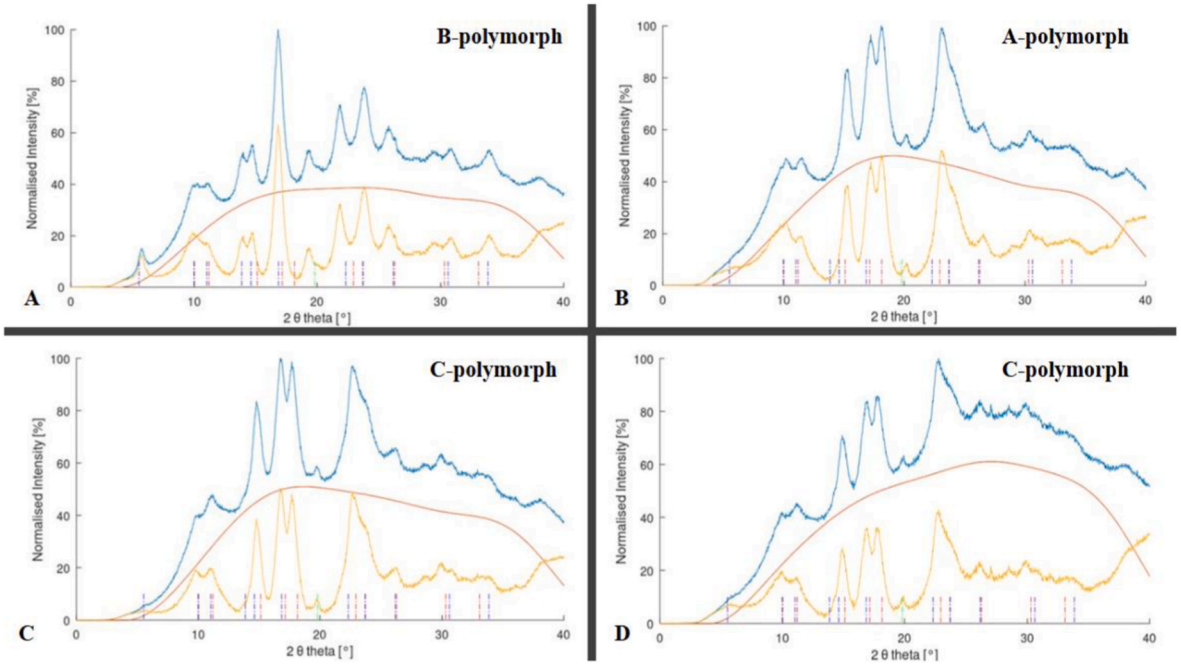

Fig. 8. A-D XRD diffractograms of potato (A), tapioca (B) sago (C) and swamp taro (D) starches hydrolysed by water. The blue signal represents the raw data from the instrument, the red signal represents the halo, and the yellow signal represents the treated signal.

(SPBBs) can be seen in the XRD results in Fig. 9 which gives the XRD diffractograms of the complete film with the gelatine, potato (A), tapioca (B), sago (C) and swamp taro (D). The blue signal represents the raw data from the instrument, the red signal represents the halo, and the yellow signal represents the treated signal. The blue and red dotted lines correspond to the polymorphic type of the samples, B and A type, respectively, with the green dotted line indicating the V-type region. Gelatine films tend to be represented on the XRD diffractogram by having a broad peak at 20°, allowing an intense peak at 28° and a smaller peak in the region of 7° to 8°. These characteristic peaks indicated the slight reconstitution of the collagen-like triple helix structure [32,49]. Soliman and Furuta [32] discussed how starch and gelatine interact in the sense that the polysaccharides' anionic starch domain interacts with the gelatine cationic domains, which can lead to the intensity of the characteristic peaks of the crystalline region of gelatine decreasing with increasing the percentage of amylopectin soluble starch in their blends. These results can be explained because the incorporation of amylopectin can block the reconstitution of the gelatine helical structure. Classically, a polymer-polymer interaction between polymer constituents of a blend is at the expense of their crystallisation process or does not favour crystalline domain formation for each pure macromolecule [32].

Based on the literature, the results from Fig. 9 occur because the starch swells on contact with water and gelatinises; during this time, the starch helix opens, allowing the gelatine and glycerol molecules to enter the double helix. During the curation or drying process, one of two outcomes was believed to occur; these molecules become trapped inside the starch, or they become confined inside the gelatine matrix, rearranging into a more prominent helix and creating different polymers based on the starch implemented in the formulation.

3.4. Goniometry

The contact angle (CA) and surface free energy (SFE) measurements provide insight into the surface hydrophobicity (CA >90°) or hydrophilicity (CA < 90°) of biopolymers. These parameters are crucial for understanding surface wettability, moisture content, and water vapour permeability, factors that influence a material's performance in specific applications like the shelf life of packaged food [13,50,51]. The evolution of the water-contact angle (WCA) according to time reveals the wetting properties of the polymer. For instance, at initial contact, all SPBBs except swamp taro exhibited WCA greater than 90°, Table 1, revealing an almost non-hydrophilic surface. At the 1-min mark, potato, tapioca, and swamp taro polymers displayed WCAs of 87.9°, 84.8° and 82°, respectively, displaying an increasing hydrophilicity (Fig. 10). Meanwhile, sago, with a WCA of 93.7°, showed hydrophobic characteristics, limiting its suitability for applications requiring water interaction, but ideal for those desiring hydrophobic qualities. Over time, as seen in Table 1 the WCA progressively decreases to below 90°, indicating that all the biopolymers become more hydrophilic due to water absorption and/or swelling, as shown in Fig. 1. A more hydrophobic surface is desirable, as noted by Żołek-Tryznowska and Kałuża [50], whose potato and tapioca polymers had WCA 55.2° and 62.9°, respectively. This is because the main drawback of starch-based films and starch-protein blend bioplastics (SPBBs) is their affinity to water, which limits their potential applications. Findings by Channa et al. [51] indicated SPBB WCA values varied from 50° to 70° (not specifying if initial or equilibrium time values of WCA) with corn as their starch of choice and fish gelatine as the protein source—Fig. 10 A and B were used as representative images for the SPBBs before baseline correction to observe how the polymers react to water droplets visually.

Compared to conventional polymers, the WCA values of SPBBs fall within a similar or slightly more hydrophilic range. HDPE and PE, for example, exhibit WCAS between 80.5° and 94.9-97.2°, respectively, with PP showing highly hydrophobic values exceeding 94.9-107.3°, Table 1. PLA and cross-linked starch demonstrate more hydrophilic behaviour with WCAs of 76.7° and 70°, respectively [13,55]. These values position the SPBBs closer to commercial bioplastics, PLA and traditional petroleum polymers, HDPE.

The surface free energy and the water contact angle are crucial parameters influencing coating, painting or ink deposition and the wettability properties of polymer films. The values of total SFE in the Żołek-Tryznowska and Kałuża [50] study were much higher for potato and tapioca, in the range of 56.5 and 53.6 mN/m, respectively. The same study reported SFE values for LDPE and PLA, as seen in Table 1, along with values for PE and PP from Wypych, pp. 370, 531 (2022). Moreover,

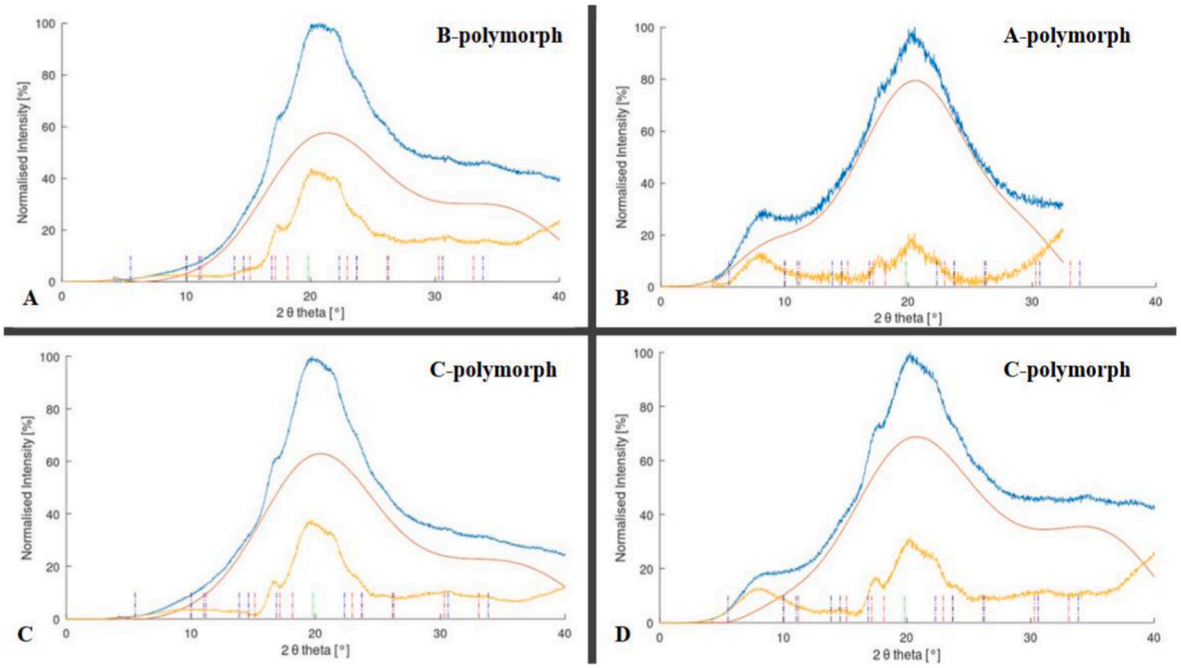

Fig. 9. A-D XRD diffractograms of the complete film with the gelatine, potato (A), tapioca (B), sago (C) and swamp taro (D). The blue signal represents the raw data from the instrument, the red signal represents the halo, and the yellow signal represents the treated signal.

Table 1
Water contact angle, critical surface tension and surface free energy of studied bioplastics and compared to commercial plastics and bioplastics.

Polymer	Water Contact Angle (°)			Critical Surface Tension (mN/m)	Surface Free Energy (mN/m)		
	0 min	1 min	3 min		Y_S^P	Y_S^D	Y_S
Potato	104.9 ± 8.9^{A}	$87.9 \pm 6.9^{A,B}$	84.7 ± 4.9^{B}	31.8	46.6	2.7	49.4
Tapioca	104.1 ± 20.3^{A}	$84.8 \pm 7.2^{A,B}$	80.9 ± 6.7^{B}	43.4	11.5	9.4	20.9
Sago	99.9 ± 5.6^{A}	$93.7 \pm 2.8^{A,B}$	87.8 ± 2.8^{B}	39.1	15.1	7.4	22.5
Swamp taro	85.6 ± 19.5	82.2 ± 15.5	76.8 ± 15.9	14.3	31.2	0.8	32.0
HDPE	80.5 [52]			26-28.8 ([53], pp.171)	39.4 [54]		
Cross-linked Starch	70 [55]			45 ([53], pp.720)	Depending on the starch used		
PP	94.9-107.3 ([53], pp.531; [56], 2019)			20.4 ([53], pp.531)	30.2 ([53], pp.531)		
PE	94.9-97.2 ([53], pp.370; [56], 2019)			35.1-37.6 ([53], pp.370)	33.5 ([53], pp.370)		
LDPE	97.7 (left angle), 99.6 (right angle) [57]			-	35.3[50]		
PLA	76.7 [13]			27.3 [13]et al.	41.6 - 49.7[50,58]		

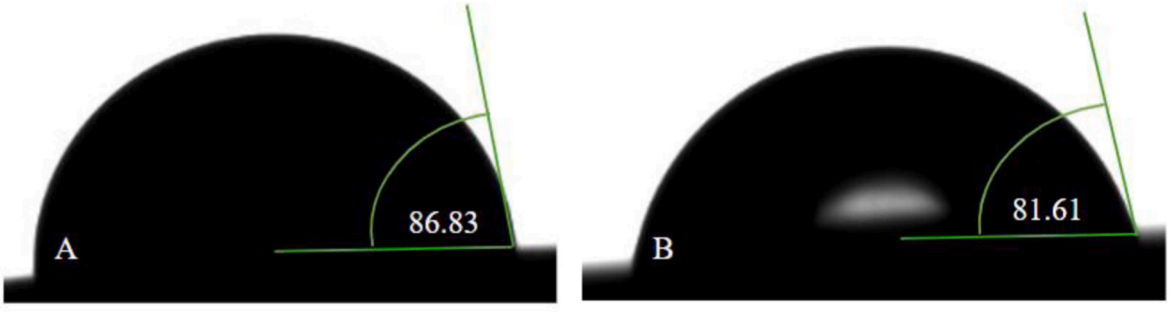

Fig. 10. Representative images of the WCA of SPBB's potato (A) and tapioca (B), respectively.

the fish gelatine polymers show surface free energy values of 53.7 mN/m^2, indicating a higher value than the SPBBS as seen in Table 1 as found by Poulain et al. [59]. Notably, potato demonstrated the highest surface energy among the SPBBs at 49.4 mN/m and has a SFE very similar to that of PLA.

Critical surface tension (CST) corresponds to the surface tension of liquids able to totally wet the surface of the concerned solid and thus spread fast. The relationship between CST and liquid spreading is vital in applications such as food packaging, where surface properties impact moisture transfer and the shelf-life of products [13]. Tapioca and sago have the highest CST with values of 43.4 and 39.1. mN.m^{-1} respectively (Table 1). This means liquids like diethylene glycol (SFE = 45 mN m^{-1}), soapy water (SFE up to 45 mN m^{-1}, for cleaning application) or benzyl alcohol (SFE = 39 mN m^{-1}) will well spread and cover the film surface. Potato, whose value is 31.8 mN m^{-1}, will be easily wet by xylene (SFE = 29 mN m^{-1}), heptanoic acid (SFE = 28 mN m^{-1}), etc. Finally, the swamp taro exhibits the lowest value corresponding to liquids like perfluoro solvents; however, the swamp taro also displayed an irregular and rough surface that may have biased the CST calculation.

The surface kinetic behaviour of the polymers when in contact with the solvents, water, glycerol, ethylene glycol, water: glycerol and water: ethylene glycol was evaluated to better understand how these polymers interact with specific polar/hydrophilic liquids, summarised in Fig. 1. These liquids were used for determining the polar and dispersive components of the surface free energy of the starch-based bioplastics (SPBBs), using the Owens and Wendt model [60]. How these solvents interact with the different SPBBs through processes such as absorption, spreading, swelling or combinations of these actions, was observed over 1 min per sample. Insights into SPBB interactions guide end-use choice, with their unique surface wettability properties, which can be leveraged to enhance performance in various applications. Tapioca polymer, exhibiting excellent wettability, is well-suited for surfaces requiring strong wetting properties. In contrast, with its water-resistant characteristics, the sago polymer is best for packaging films that need moisture protection. Lastly, the swamp taro polymer is useful for selective applications where controlled water interaction is desired. It has to be noted that the potato starch is highly refined compared to other starches and thus may not contain a significant amount of protein that may induce an increase of dispersive forces, thus a lower SFE.

3.5. *Water vapour and O_2 permeability*

Water Vapour Permeability (WVP) refers to the rate at which water vapour permeates through a material under a water vapour partial pressure gradient. The WVP of blend films is exposed in Fig. 11. Several studies have explored the WVP of starch-based films, offering valuable insights into polymer-solute interactions [61]. WVP is one of the most extensively studied properties of films due to its significance in determining the behaviour of different polymers toward liquid water and/or water vapour during storage [47]. Like most biopolymers, the WVP of starch films are influenced by various factors, including starch type,

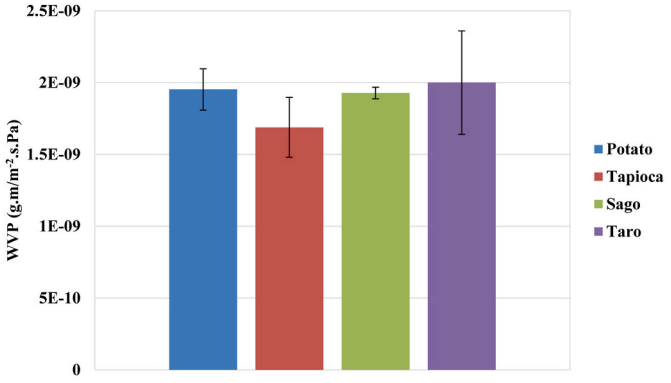

Fig. 11. Water Vapour Permeability (WVP) of biopolymers, potato, tapioca, sago and swamp taro (Values represent the mean of N = 5 (each sample), ±standard deviation. Using a value of P > 0.05, ANOVA and Tukey-Kramer analysis were conducted on this data.

presence of plasticisers, and environmental conditions [50,62]. For example, WVP in tapioca films increase with the glycerol concentration, ranging from 10 to 20 % w/w; however, at 30 % w/w, WVP decreases due to the higher glycerol content, causing an anti-plasticising effect [47,63]. Glycerol and water, small hydrophilic molecules, likely insert themselves into the adjacent polymer chains, enhancing the mobility within the film matrix [47].

Regarding performance, no statistically significant difference between the WVP of the different starches used was observed in the SPBBs, Fig. 11; however, there are some notable differences compared to the literature. For instance, a potato-based film by Fakhouri et al. [64] reported a WVP value of 0.15×10^{-9} g m m^{-2}.s^{-1}.Pa^{-1}, which produced lower WVP than the 1.95×10^{-9} g m.m^{-2}.s^{-1}.Pa^{-1}obtained in this study. Compared to conventional plastics such as HDPE (7.2×10^{-14} g m m^{-2}.s^{-1}.Pa^{-1}), LDPE (5.5×10^{-13} g m m^{-2}.s^{-1}.Pa^{-1}), and PLA (9×10^{-11} g m m^{-2}.s^{-1}.Pa^{-1}) [53] SPBBs films have much poorer barrier properties to moisture as expected. Compared to gelatine-based polymers like those discussed in Poulain et al., (2025), the SPBBs display similar water vapour permeability properties. The difference in barrier properties could be attributed to the variety of starches utilised, or over-plasticization of the SPBBs by the glycerol and water that enhances the moisture absorption and, thus, swelling during WVP measurement, allowing for increased water transmission.

The presence of oxygen is a primary factor contributing to the efficiency, quality, and safety of packaged foods, reducing food spoilage. Oxygen is a major contributor to food spoilage, with high moisture content promoting the growth of aerobic microorganisms in fresh food packaging [65]. Consequently, oxygen (O_2) barrier properties of the packaging films are critical in determining their effectiveness for food applications. Many studies have demonstrated that biobased polymer composition and structure modifications can significantly alter their barrier properties. Incorporating gelatine into blended biopolymer films has improved their barrier properties, reducing the permeability of O_2 and CO_2 as gelatine content increases [63]. Starch-based films have also exhibited strong O_2 and CO_2 barrier properties, reinforcing their potential for sustainable packaging materials [66]. According to Wang et al. [49], the addition of various starches has been found to decrease O_2 permeability, with the lowest value observed in corn films. Furthermore, Wang et al. [49] found that the SPBB they created resulted in a lower O_2 permeability value compared to that of pure bovine gelatine bioplastics, suggesting that starch enhances the barrier-resistant properties of gas exchange.

From the data presented in Fig. 12, the oxygen permeability of gelatine-starch based films ranges from about 1000 to 4000 cm^3 µm m^{-2}.day^{-1}.bar^{-1}. Overall, when compared to classical synthetic polymers with the same units such as HDPE (25600 cm^3 µm m^{-2}.day^{-1}.bar^{-1}), LDPE (187 000), PP (61 000) and PLA (90 000) [53], the SPBBs generally present one to two order of magnitude more performing system against O_2 transfers in moderated humidity conditions. Tapioca exhibited statistically significantly lower O_2 permeability than that of swamp taro. Both potato and sago SPBBs demonstrated moderate O_2 permeability and, consequently, moderate barrier properties; these materials would be suited to less oxygen-sensitive applications. In contrast, tapioca SPBB showed the lowest O_2 permeability among the tested SPBBs, indicating the best relative O_2 barrier performance compared the other SPBBs, making it ideal for potential applications such as food packaging. Swamp taro allowed for the most O_2 to pass through, indicating poorer gas barrier properties, and would suit an application as barrier packaging or controlled oxygen transmission applications (e.g., for fresh produce). These barrier properties are critical for specific sectors, such as food packaging applications, where adequate moisture and oxygen control can significantly extend shelf-life, maintain food quality, and ensure safety by reducing the growth of aerobic microorganisms.

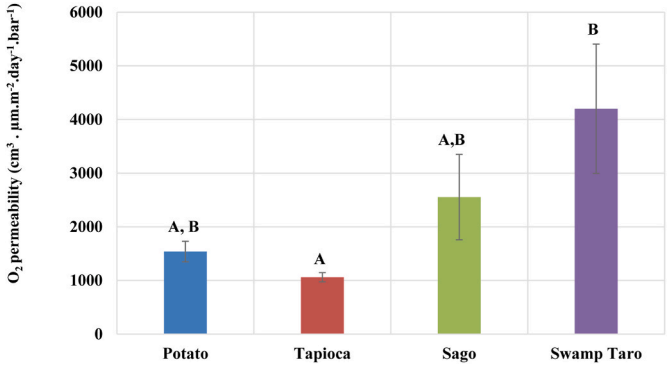

Fig. 12. O_2 permeability at 50% RH of the SPBBs (potato, sago and swamp taro), respectively, with different scripture letters indicating different levels of significance, values represent the mean of N = 3 (each sample), ±standard deviation using a value of $P < 0.05$, except for tapioca which was completed in duplicate, bars with same letters are not significantly different).

3.6. DMTA

Dynamic mechanical thermal analysis (DMTA) tests are conducted to measure glass transition, tan delta, loss modulus and storage modulus of different materials [67]. The glass transition temperature (Tg) is when a material shifts from a rigid, glassy state to a more rubber-like state [68]. For a viscoelastic polymer, two moduli can be distinguished: storage modulus (E′), which measures the elastic behaviour or stiffness of the material, and loss modulus (E″), which represents the energy dissipation as heat due to internal friction of the material [67,69]. Tan delta is defined as the ratio of the loss modulus to the storage modulus, highlighting the damping behaviour of the material [67,70].

From the data showcased in Table 2 regarding the Tg of the SPBBs, they all fall into the Tg range of starch-based polymers at −55 °C, according to Wypych [53]. Sago-based SPBB has the lowest Tg, indicating ductility at lower temperatures, whereas tapioca and potato-based SPBBs have higher Tg values, showing relatively higher rigidity. Considering the Tg of pure starch, whose value is about 332 °C [71], and that of undried gelatine at about 55 °C [72], it was demonstrated that the SPBB are over-plasticised by the glycerol (33.3% of the dry weight), the absorbed water and maybe the gelatine. Plasticiser content, particularly water, strongly affects Tg. Indeed, Liu et al. [73] displayed a tremendous decrease in the Tg of starch with moisture content, in which the Tg value drops to 50-80 °C according to starch type and amylose/amylopectin ratio for 13% of moisture content. The sago SPBB, with its lower Tg, may be suitable for materials requiring impact resistance at low temperatures.

The tan Delta at the Tg showed statistically significant differences between the polymers, with potato and tapioca SPBBs having lower values than sago SPBB (Table 2). A higher tan delta suggests better energy dissipation and higher damping ability, meaning it absorbs and dissipates energy well; this might be due to higher plasticization and thus higher mobility in the material, potentially being functional as a shock-absorbing layer. All the SPBB's results were higher than those of PP, HDPE and LDPE, according to Wypych [53], which was valued at 0.0005 for PP, and HDPE and LDPE have values of 0.002 Tan delta at 1 Hz. This indicates that the polymers from this study have greater energy dissipation ability than traditional plastics.

Tapioca SPBB exhibited the highest loss modulus (E″), suggesting greater energy dissipation and viscous flow at the Tg, Table 2. In contrast, sago SPBB showed the lowest loss modulus, suggesting lower viscous behaviour and reduced energy dissipation. Similarly, the storage modulus (E′) for tapioca-based SPBB had the highest value, whereas sago films exhibited a softer structure. Both moduli decreased across all SPBBs as the temperature increased, indicating a transition towards a softer polymer at ambient temperature. At 25 °C, potato and tapioca SPBBs modulus values approach those of other polymers, like PP, with a

Table 2
Results from DMTA with Tg, Tan Delta, loss and storage moduli at Tg and room temperature.

Sample SPBB	Tg (°)	Tan Delta at Tg	Loss modulus (MPa) at Tg	Storage modulus (MPa) at Tg	Loss modulus (MPa) at 25 °C	Storage modulus (MPa) at 25 °C
Potato	-45.1 ± 2.2^{A}	0.159 ± 0.015^{A}	$936.3 \pm 246.4^{A,B}$	$5744.3 \pm 1037.9^{A,B}$	$134.3 \pm 54.2^{A,B}$	906.5 ± 346.5^{A}
Tapioca	-43.3 ± 1.6^{A}	0.178 ± 0.016^{A}	1573.8 ± 817.4^{A}	8607.5 ± 3659.9^{A}	228.0 ± 76.5^{A}	1087.0 ± 284.4^{A}
Sago	-51.7 ± 2.1^{B}	0.210 ± 0.007^{B}	344.3 ± 57.1^{B}	1633.0 ± 218.5^{B}	20.3 ± 4.0^{B}	73.5 ± 17.3^{B}

Values represent averages of N = 4 ± std except for biopolymers generated with Sago with N = 3 ±std with different script letters indicating different significance levels. Swamp taro data was not available at the time.

value of ~1000 MPa [74], suggesting moderate rigidity. In contrast, sago SPBB had rigid behaviour, making it potentially suitable for materials with low-stress applications. Although compared to PLA at ~250 MPa at 30 °C [75], SPBBs are more flexible, they are not as soft in comparison to PP at ~ 80 MPa at 25 °C [74]. It is essential to clarify that these comparisons are limited due to structural differences among the polymers, and so are rough comparisons. However, the decreasing trend of both E' and E'' supports the classification of SPBBs as bendable biopolymers.

4. Conclusion

In conclusion, this study evaluated the functional properties of SPBBs derived from various sources – potato, tapioca, sago and swamp taro – focusing on how starch sources influence the chemical composition, surface characteristics and barrier properties. The results indicated no significant difference between the percentage ratio of amylose and amylopectin, and these results fell within the normal range reported in the literature. FTIR analysis revealed that while the starches had subtle differences in their profiles in the O-H region, incorporating the fish gelatine, water, and glycerol homogenised them, resulting in nearly identical profiles. This suggests a good level of compatibility between the starches, glycerol and protein matrix, with gelatine contributing functional amide bands and polar groups capable of forming hydrogen bonds within the polymer network. The XRD analysis of the raw starches demonstrated distinct polymorphic structures, with potato classified as B-polymorph, tapioca as A-polymorph, and sago and swamp taro as C-polymorphs. Blending the starch double-helix and gelatine triple-helix was found to disrupt the reconstitution of the polymer, and the distinctive polymorph peaks were no longer present in the final SPBB films. The disappearance or broadening of these peaks aligned with the FTIR evidence of intermolecular bonding among the various polymer components. Surface properties analysis revealed that higher SFE correlates with better wettability, as observed in potato SPBB. In contrast, lower SFE and CST values in sago and swamp taro SPBBs indicate hydrophobic surfaces essential in various applications, such as coatings and food packaging. This behaviour of the polymers suggests that the difference in starch influenced this conduct, likely related to the availability of polar groups identified in the FTIR. Regarding the barrier properties of the polymers, the SPBBs displayed poor water barrier properties compared to traditional polymers. Concerning O_2 permeability, tapioca SPBB emerged as the most promising candidate for oxygen-sensitive applications like food packaging. However, the SPBBs do not meet the desired oxygen permeability standards compared to established polymers. The DMTA findings indicated that the SPBBs vary in rigidity depending on starch type. Tapioca SPBB was the stiffest; in contrast, sago SPBB showed soft behaviour. This trend aligns with the barrier, where more rigid polymers exhibited better oxygen resistance. The results showed that although starches share broadly similar chemical compositions, the starch type impacts the overall SPBBs properties. By evaluating FTIR, XRD, goniometry, permeability and DMTA data, this study highlights the complex interplay between starch type, gelatine, and plasticisers in determining the final properties of bioplastics. It indicates further insight into the molecular network organisation between starch and gelatine.

Despite the similarity in starch amylose/amylopectin composition, the resulting SPBBs exhibited notable variations in surface and barrier performance, indicating other factors such as granule morphology or the presence of minor companies, including lipids, may influence the material. Moreover, the gelatin-starch interactions, not directly related to amylose/amylopectin ratio but to the polymorphism of starch, induced performance differences according to the starch type (as supposed from XRD data) as it changed the network (ratio between helix and random coil of gelatin). Such insights could deepen the understanding of these networks and aid in formulation to create a wide range of potential applications, such as food packaging or agricultural films, where controlled permeability and flexibility are essential.

Fundings

This research was mainly supported by grants from the South East Technological University President Award Fellowship grant, funding number PES 1393, and the ERASMUS traineeship grant for the Irish partner. For the French partner, this work was partly supported by the Conseil Régional de Bourgogne Franche-Comté and the European Union through the PO FEDER-FSE Bourgogne 2021-2027 programs who invest in lab equipment.

CRediT authorship contribution statement

Jade Stanley: Conceptualization, Data curation, Formal analysis, Investigation, Methodology, Resources, Software, Validation, Visualization, Writing – original draft, Writing – review & editing. **Clément Poulain:** Conceptualization, Data curation, Formal analysis, Investigation, Methodology, Resources, Validation, Visualization, Writing – original draft, Writing – review & editing. **Frédéric Debeaufort:** Conceptualization, Formal analysis, Funding acquisition, Methodology, Project administration, Resources, Supervision, Validation, Writing – review & editing. **Claire-Hélène Brachais:** Conceptualization, Formal analysis, Methodology, Resources, Supervision, Validation, Writing – review & editing. **David Culliton:** Conceptualization, Project administration, Supervision, Validation, Writing – review & editing. **Nasreddine Benbettaieb:** Conceptualization, Supervision, Validation, Writing – review & editing. **Antonio-Jonay Jovani-Sancho:** Conceptualization, Supervision. **Adriana Cunha Neves:** Conceptualization, Funding acquisition, Project administration, Supervision, Writing – review & editing.

Declaration of competing interest

The authors declare that they have no known competing financial interests or personal relationships that could have appeared to influence the work reported in this paper.

Acknowledgements

The authors thank Bernadette Rollin and Agathe Pissis, from UMR PAM, and Marie-Laure Léonard and Jean-Pierre Couvercelle from Polytech Dijon for access and for helping with some equipment. This work has benefited from and contributed to the knowledge and skills acquired

and shared within the PropackFood, the French scientific and technological joint network (RMT) lead by ACTIA.

Data availability

Data will be made available on request.

References

[1] J. Stanley, D. Culliton, A.J. Jovani-Sancho, A.C. Neves, The journey of plastics: historical development, environmental challenges, and the emergence of bioplastics for single-use products, Eng—Advances in Engineering (2025), https://doi.org/10.3390/eng6010017.

[2] E.M. Melchor-Martínez, R. Macías-Garbett, L. Alvarado-Ramírez, R.G. Araújo, J. E. Sosa-Hernández, D. Ramírez-Gamboa, L. Parra-Arroyo, A.G. Alvarez, R.P. B. Monteverde, K.A.S. Cazares, A. Reyes-Mayer, M.Y. Lino, H.M.N. Iqbal, R. Parra-Saldívar, Towards a circular economy of plastics: an evaluation of the systematic transition to a new generation of bioplastics, Polymers (2022), https://doi.org/10.3390/polym14061203. (Accessed 13 September 2024).

[3] J. Stanley, D. Culliton, A.-J. Jovani-Sancho, A.C. Neves, Mechanical properties of starch-protein blend bioplastics, World J. Eng. Res. Tech 8 (12) (2022) [online] 2022 Available at: https://www.wjert.org/home/article_abstract/1301. (Accessed 27 March 2023).

[4] M. Maulida, M. Siagian, P. Tarigan, Production of starch based bioplastic from Cassava peel reinforced with microcrystalline celllulose Avicel PH101 using sorbitol as plasticizer, J. Phys., Conf. Ser. (2016), https://doi.org/10.1088/1742-6596/710/1/012012.

[5] T.D. Moshood, G. Nawanir, F. Mahmud, F. Mohamad, M.H. Ahmad, A. AbdulGhani, Expanding policy for biodegradable plastic products and market dynamics of bio-based plastics: challenges and opportunities, Sustainability (2021), https://doi.org/10.3390/su13116170. (Accessed 4 October 2024).

[6] European bioplastics, Bioplastics, 2019 [online] European Bioplastics e.V. Available at: https://www.european-bioplastics.org/bioplastics/.

[7] M.L. Di Lorenzo, A. Longo, R. Androsch, Polyamide 11/Poly(butylene succinate) bio-based polymer blends, Materials 12 (17) (2019) 2833, https://doi.org/10.3390/ma12172833 [online]. (Accessed 26 March 2025).

[8] K.Y. Perera, A.K. Jaiswal, S. Jaiswal, Biopolymer-based sustainable food packaging materials: challenges, solutions, and applications, Foods (2023), https://doi.org/10.3390/foods12122422.

[9] J. Muller, C. González-Martínez, A. Chiralt, Review Combination of Poly(Lactic) Acid and Starch for Biodegradable Food Packaging, 2017.

[10] N.A. Ismail, S. Mohd Tahir, Y. Norihan, M.F. Abdul Wahid, N.E. Khairuddin, I. Hashim, N. Rosli, M.A. Abdullah, Synthesis and characterization of biodegradable starch-based bioplastics, Mater. Sci. Forum 846 (2016) 673–678, https://doi.org/10.4028/www.scientific.net/msf.846.673 [online].

[11] R.J. Hynes Navasingh, M.K. Gurunathan, M.P. Nikolova, J.B. Królczyk, Sustainable bioplastics for food packaging produced from renewable natural sources, Polymers 15 (18) (2023) 3760, https://doi.org/10.3390/polym15183760 [online].

[12] A.C. Neves, T. Ming, M. Mroczkowska, D. Culliton, The effect of different starches in the environmental and mechanical properties of starch blended bioplastics, Adv. Sci. Technol. Eng. Syst. J. 5 (6) (2020) 550–554, https://doi.org/10.25046/aj050666 [online].

[13] A. Božović, K. Tomašević, N. Benbettaieb, F. Debeaufort, Influence of surface Corona discharge process on functional and antioxidant properties of bio-active coating applied onto PLA films, Antioxidants 12 (4) (2023) 859, https://doi.org/10.3390/antiox12040859 [online].

[14] E. Basiak, M. Geyer, F. Debeaufort, A. Lenart, M. Linke, Relevance of interactions between starch-based coatings and plum fruit surfaces: a physical-chemical analysis, Int. J. Mol. Sci. 20 (9) (2019) 2220, https://doi.org/10.3390/ijms20092220 [online].

[15] Z. Zhang, W. Wang, A.N. Korpacz, C.R. Dufour, Z.J. Weiland, C.R. Lambert, M. T. Timko, Binary liquid mixture contact-angle measurements for precise estimation of surface free energy, Langmuir 35 (38) (2019) 12317–12325, https://doi.org/10.1021/acs.langmuir.9b01252 [online]. (Accessed 15 April 2025).

[16] W.A. Zisman, Contact angle, wettability, and adhesion, [online] Advances in chemistry series, American Chemical Society (1964), https://doi.org/10.1021/ba-1964-0043.

[17] C.J. van Oss, Development and applications of the interfacial tension between water and organic or biological surfaces, Colloids Surf. B Biointerfaces 54 (1) (2007) 2–9, https://doi.org/10.1016/j.colsurfb.2006.05.024 [online].

[18] F. Debeaufort, M. Martin-Polo, A. Voilley, Polarity homogeneity and structure affect water vapor permeability of model edible films, J. Food Sci. 58 (2) (1993) 426–429, https://doi.org/10.1111/j.1365-2621.1993.tb04290.x [online].

[19] International Standard Organisation (2017). ISO 2528:2017. [online] ISO. Available at: https://www.iso.org/standard/72382.html [Accessed 4 April. 2025].

[20] International Standard Organisation (2007). ISO 15105-1:2007. [online] ISO. Available at: https://www.iso.org/standard/41677.html [Accessed 28 March. 2025].

[21] M. Riaz, Snack Foods: Processing, 2016 [online] sciencedirect. Available at: https://www.sciencedirect.com/science/article/pii/B9780123944375001601. (Accessed 6 August 2021).

[22] Duan, D., Donner, E., Liu, Q., Smith, D. and Ravenelle, F., 2012. Potentiometric titration for determination of amylose content of starch – a comparison with colorimetric method. [online] sciencedirect. Available at: https://www.sciencedirect.com/science/article/pii/S030881461101168X?casa_token=wTozdzRF_BUAAAAA:Sl8qoABUn1VjTnivouafXcfevd7XpbefYqK4XVLnAOBScqi7B0yeuL3eQDSnbwEUiNSR2WTRgBE [Accessed 6 August 2021].

[23] S. Gunawan, H. Aparamarta, R. Darmawan, I. Zarkasie, W. Prihandini, Effect of initial bacteria cells number and fermentation time on increasing nutritive value of sago flour, Malays. J. Fundam. Appl. Sci 14 (2289-5981) (2018) 246–250. https://www.semanticscholar.org/paper/Effect-of-initial-bacteria-cells-number-and-time-on-Gunawan-Aparamarta/5c654a86157053e523fe450f56cf5ff447815b6e.

[24] D. Adawiyah, T. Sasaki, K. Kohyama, Characterization of arenga starch in comparison with sago starch [online], ScienceDirect (2013). Available at: https://www.sciencedirect.com/science/article/pii/S0144861712012337?pes=vor. (Accessed 4 August 2021).

[25] R. Nguimbou, H. Himeda, N. Njintang, L. Tatsadjieu, B. Facho, J. Scher, C. Mbofung, Comparative physicochemical, thermal and microstructural properties of starches from two underutilized Taro ecotypes, Int. J. Biosci. 2 (4) (2012) 64–74 [online] Available at: https://www.semanticscholar.org/paper/Comparative-physicochemical%2C-thermal-and-properties-Nguimbou-Himeda/d3bb47588f1d365c4847e4326f130e5121d02f61. (Accessed 30 August 2021).

[26] E. Pérez, F. Schultz, E. Delahaye, Characterization of Some Properties of Starches Isolated from Xanthosoma sagittifolium (Tannia) and Colocassia Esculenta (Taro), 2005 [online] Sciencedirect. Available at: https://www.sciencedirect.com/science/article/pii/S0144861704004618?casa_token=s9xuCLtleZkAAAAA:_N9ZZypE1UGFiiVC8_l2B10mD4-gRCm0CoeZbi7rdu6QlpZw_NNb1Tv6qsUDLp1aNQ0ydDA-ZDk. (Accessed 30 August 2021).

[27] J. Tattiyakul, P. Pradipasena, S. Asavasaksakul, Taro Colocasia esculenta (L.) Schott Amylopectin Structure and Its Effect on Starch Functional Properties [online], Wiley Online Library, 2007. Available at: https://onlinelibrary.wiley.com/doi/abs/10.1002/star.200700620. (Accessed 30 August 2021).

[28] Stawski, D., 2008. New determination method of amylose content in potato starch. [online] Available at: <https://www.sciencedirect.com/science/article/pii/S0308814608003038?via=ihub>[Accessed 5 August 2021].

[29] Saiful, H. Helwati, S. Saleha, T. Iqbalsyah, Development of bioplastic from wheat Janeng starch for food packaging [online], Iopscience (2019). iop.org. Available at: https://iopscience.iop.org/article/10.1088/1757-899X/523/1/012015/meta. (Accessed 14 October 2021). iop.org/article/10.1088/1757-899X/523/1/012015/meta> [Accessed 14 October 2021].

[30] B.H. Ayalke, D.E. Woldemichael, Experimental analyses of eco-friendly plasticizer on taro starch-based bioplastic for injera packing application, Research Square (2022), https://doi.org/10.21203/rs.3.rs-2188198/v1 [online].

[31] S. Nakajima, S. Horiuchi, A. Ikehata, Y. Ogawa, Determination of starch crystallinity with the Fourier-transform terahertz spectrometer, Carbohydr. Polym. 262 (2021) 117928, https://doi.org/10.1016/j.carbpol.2021.117928 [online]. (Accessed 16 April 2025).

[32] E.A. Soliman, M. Furuta, Influence of phase behavior and miscibility on mechanical, thermal and micro-structure of soluble starch-gelatin thermoplastic biodegradable blend films, Food Nutr. Sci. 5 (11) (2014) 1040–1055, https://doi.org/10.4236/fns.2014.511115 [online].

[33] H. Omrani-Fard, M. Abbaspour-Fard, M. Khojastehpour, A. Dashti, Gelatin/Whey Protein- Potato Flour Bioplastics: Fabrication and Evaluation [online], SpringerLink, 2020. Available at: https://link.springer.com/article/10.1007/s10924-020-01748-1. (Accessed 14 October 2021).

[34] Asrofi, M., Syafri, E. and Sujito, 2019. Moisture resistance of sugarcane bagasse cellulose filled tapioca starch biocomposites: effect of cellulose loading. [online] Ijpsat.es. Available at: <http://ijpsat.es/index.php/ijpsat/article/view/1444> [Accessed 22 October 2021].

[35] M. Mroczkowska, D. Culliton, K. Germaine, A.C. Neves, Comparison of mechanical and physicochemical characteristics of potato starch and gelatine blend bioplastics made with gelatines from different sources, Clean Technol. 3 (2) (2021) 424–436, https://doi.org/10.3390/cleantechnol3020024 [online].

[36] E. Baggio, B.S. Scopel, M. Rosseto, A. Dettmer, C. Baldasso, Transglutaminase effect on the gelatin-films properties, Research Square (Research Square) (2021), https://doi.org/10.21203/rs.3.rs-179633/v1 [online]. (Accessed 17 April 2025).

[37] E.L. Hanry, N.F.M. Redzwan, N.F.A.K. Badeges, N. Surugau, Characterization of biofilms developed from alginate extracted from Padina sp. incorporated with calcium chloride (CaCl2), J. Phys. Conf. 2314 (1) (2022) 012022, https://doi.org/10.1088/1742-6596/2314/1/012022 [online].

[38] A.A. Olagundoye, A.O. Adejuwon, Characterization of potato peel starchbased bioplastic reinforced with banana pseudostem cellulose for packaging, applications| International Journal of Innovative Science and Research Technology (2023) [online] Ijisrt.com. Available at: https://ijisrt.com/characterization-of-potato-peel-starchbased-bioplastic-reinforced-with-banana-pseudostem-cellulose-for-packaging-applications. (Accessed 8 October 2024).

[39] Z. Li, M. Wu, W. Wei, Y. An, Y. Li, Q. Wen, D. Zhang, J. Zhang, C. Yao, Q. Bi, D. Guo, Fingerprinting evaluation and gut microbiota regulation of polysaccharides from Jujube (Ziziphus jujuba Mill.) fruit, Int. J. Mol. Sci. 24 (8) (2023) 7239, https://doi.org/10.3390/ijms24087239 [online].

[40] E. Syafri, A. Kasim, H. Abral, A. Asben, Effect of precipitated calcium carbonate on physical, mechanical and thermal properties of cassava starch bioplastic composites [online], Researchgate (2017). Available at: https://www.researchgate.net/publication/320748469_Effect_of_Precipitated_Calcium_Carbonate_on_Physical_Mechanical_and_Thermal_Properties_of_Cassava_Starch_Bioplastic_Composites. (Accessed 22 October 2021).

[41] F.J. Warren, M.J. Gidley, B.M. Flanagan, Infrared spectroscopy as a tool to characterise starch ordered structure—a joint FTIR–ATR, NMR, XRD and DSC

study, Carbohydr. Polym. 139 (2015) 35–42, https://doi.org/10.1016/j.carbpol.2015.11.066 [online].
[42] R.A. Talja, M. Peura, R. Serimaa, K. Jouppila, Effect of amylose content on physical and mechanical properties of potato-starch-based edible films, Biomacromolecules 9 (2) (2008) 658–663, https://doi.org/10.1021/bm700654h [online].
[43] A. Lopez-Rubio, B.M. Flanagan, E.P. Gilbert, M.J. Gidley, A novel approach for calculating starch crystallinity and its correlation with double helix content: a combined XRD and NMR study, Biopolymers 89 (9) (2008) 761–768, https://doi.org/10.1002/bip.21005 [online].
[44] C. Mutungi, L. Passauer, C. Onyango, D. Jaros, H. Rohm, Debranched cassava starch crystallinity determination by Raman spectroscopy: correlation of features in Raman spectra with X-ray diffraction and 13C CP/MAS NMR spectroscopy, Carbohydr. Polym. 87 (1) (2012) 598–606, https://doi.org/10.1016/j.carbpol.2011.08.032 [online].
[45] M. Todica, N. Cioica, L.E. Olar, I. Papuc, C. Cota, E. Marin, D. Manea, E.M. Nagy, Preliminary XRD and IR investigation of some starch based biodegradable systems, Rom. Biotechnol. Lett 21 (5) (2016) 11825–11831 [online], https://www.researchgate.net/publication/309740640_Preliminary_XRD_and_IR_investigation_of_some_starch_based_biodegradable_systems.
[46] R. Santhosh, J. Ahmed, R. Thakur, P. Sarkar, Starch-based edible packaging: rheological, thermal, mechanical, microstructural, and barrier properties – a review, Sustain. Food Technol. 2 (2) (2024) 307–330, https://doi.org/10.1039/D3FB00211J [online].
[47] P. Piyawatakarn, C. Limmatvapirat, P. Sriamornsak, M. Luangtana-Anan, J. Nunthanid, S. Limmatvapirat, Effect of glycerol on properties of tapioca starch-based films, Adv. Mater. Res. 1060 (2014) 128–132, https://doi.org/10.4028/www.scientific.net/amr.1060.128 [online].
[48] M. Schirmer, M. Jekle, T. Becker, Starch gelatinisation and its complexity for analysis, Starch - Stärke 67 (1-2) (2014) 30–41, https://doi.org/10.1002/star.201400071 [online].
[49] K. Wang, W. Wang, R. Ye, J. Xiao, Y. Liu, J. Ding, S. Zhang, A. Liu, Mechanical and barrier properties of maize starch-gelatin composite films: effects of amylose content, J. Sci. Food Agric. 97 (11) (2017) 3613–3622, https://doi.org/10.1002/jsfa.8220 [online].
[50] Z. Żołek-Tryznowska, A. Kałuża, The influence of starch origin on the properties of starch films: packaging performance, Materials 14 (5) (2021) 1146, https://doi.org/10.3390/ma14051146 [online].
[51] I.A. Channa, J. Ashfaq, M.A. Siddiqui, A.D. Chandio, M.A. Shar, A. Alhazaa, Multi-shaded edible films based on gelatin and starch for the packaging applications, Polymers 14 (22) (2022) 5020, https://doi.org/10.3390/polym14225020 [online].
[52] V. Daniloska, J. Blazevska-Gilev, V. Dimova, R. Fajgar, R. Tomovska, UV light induced surface modification of HDPE films with bioactive compounds, Appl. Surf. Sci. 256 (7) (2009) 2276–2283, https://doi.org/10.1016/j.apsusc.2009.10.052 [online].
[53] G. Wypych, Handbook of Polymers, third ed., Elsevier, 2022, pp. 171–720, 174, 193, 350, 370, 531, 480.
[54] H. Krump, A.S. Luyt, J.A. Molefi, Changes in free surface energy as an indicator of polymer blend miscibility, Mater. Lett. 59 (4) (2004) 517–519, https://doi.org/10.1016/j.matlet.2004.10.039 [online].
[55] M.K. Marichelvam, M. Jawaid, M. Asim, Corn and rice starch-based bio-plastics as alternative packaging materials, Fibers 7 (4) (2019) 32, https://doi.org/10.3390/fib7040032 [online].
[56] Accudynetest.com. (2019). Critical surface tension and contact angle with water for various polymers (sort by contact angle). [online] Available at: https://www.accudynetest.com/polytable_03.html?sortby=contact_angle [Accessed 10 April. 2025].
[57] N.N. Rohidi, S.A. Othman, Investigate the properties of different irradiated starch bioplastic for packaging application, Malays. J. Sci. 43 (1) (2024) 59–71, https://doi.org/10.22452/mjs.vol43no1.6 [online].
[58] O. Yousefzade, J. Jeddi, E. Vazirinasab, H. Garmabi, Poly(lactic acid) phase transitions in the presence of nano calcium carbonate: opposing effect of nanofiller on static and dynamic measurements, J. Thermoplast. Compos. Mater. 32 (3) (2018) 312–327, https://doi.org/10.1177/0892705718759386 [online].
[59] C. Poulain, C.-H. Brachais, A. Krystianiak, O. Heintz, M.-L. Léonard, N. Benbettaieb, F. Debeaufort, Changes in the structure and barrier properties induced by corona atmospheric plasma process applied on wet gelatin layers for packaging film applications, Food Hydrocoll. 160 (2025) 110858, https://doi.org/10.1016/j.foodhyd.2024.110858 [online].
[60] D.K. Owens, R.C. Wendt, Estimation of the surface free energy of polymers, J. Appl. Polym. Sci. 13 (8) (1969) 1741–1747, https://doi.org/10.1002/app.1969.070130815 [online].
[61] M.A. Bertuzzi, E.F. Castro Vidaurre, M. Armada, J.C. Gottifredi, Water vapor permeability of edible starch based films, J. Food Eng. 80 (3) (2007) 972–978, https://doi.org/10.1016/j.jfoodeng.2006.07.016 [online].
[62] A.A.B.A. Mohammed, A.A.B. Omran, Z. Hasan, R.A. Ilyas, S.M. Sapuan, Wheat biocomposite extraction, structure, properties and characterization: a review, Polymers (2021), https://doi.org/10.3390/polym13213624.
[63] Q. Zhong, W. Xia, Physicochemical properties of edible and preservative films from Chitosan/Cassava starch/gelatin blend plasticized with glycerol, Food Technol. Biotechnol. (2008) [online]. Available from: https://hrcak.srce.hr/26375 [Accessed Dec 2024].
[64] F.M. Fakhouri, L.C.B. Fontes, P.V. de M. Gonçalves, C.R. Milanez, C.J. Steel, F. P. Collares-Queiroz, Filmes e coberturas comestíveis compostas à base de amidos nativos e gelatina na conservação e aceitação sensorial de uvas Crimson, Food Sci. Technol. 27 (2007) 369–375, https://doi.org/10.1590/S0101-20612007000200027 [online].
[65] A.A. Arman Alim, S.S. Mohammad Shirajuddin, F.H. Anuar, A review of nonbiodegradable and biodegradable composites for food packaging application, J. Chem. 2022 (2022) 1–27, https://doi.org/10.1155/2022/7670819 [online]. (Accessed 15 April 2025).
[66] D.D. Siskawardani, Hidayat R. Warkoyo, Sukardi, Physic-mechanical properties of edible film based on taro starch (Colocasia esculenta L. Schoott) with glycerol addition, IOP Conf. Ser. Earth Environ. Sci. 458 (1) (2020) 012039, https://doi.org/10.1088/1755-1315/458/1/012039 [online].
[67] R.A. de Graaf, A.P. Karman, L.P.B.M. Janssen, Material properties and glass transition temperatures of different thermoplastic starches after extrusion processing, Starch - Stärke 55 (2) (2003) 80–86, https://doi.org/10.1002/star.200390020 [online].
[68] Greene, J.P. (2021). Glass transition temperature (Tg) - an overview | ScienceDirect topics. [online] www.sciencedirect.com. Available at: https://www.sciencedirect.com/topics/engineering/glass-transition-temperature-tg [Accessed 5 February. 2025].
[69] Y.I. Cornejo-Ramírez, O. Martínez-Cruz, C.L. Del Toro-Sánchez, F.J. Wong-Corral, J. Borboa-Flores, F.J. Cinco-Moroyoqui, The structural characteristics of starches and their functional properties, CyTA - J. Food 16 (1) (2018) 1003–1017, https://doi.org/10.1080/19476337.2018.1518343 [online].
[70] Ajiya, D.A.A., Jikan, S.S.J., Haji A. Talip, B.H.H.A.T., Badarulzaman, N.A.B., H. M, M.-P.H.M., Derawi, D.D. and Yahaya, S.Y. (2017). The influence of glycerol on mechanical, thermal and morphological properties of thermoplastic tapioca starch film. [online] publisher uthm. Available at: https://publisher.uthm.edu.my/ojs/index.php/JST/article/view/2054 [Accessed 28 January. 2025].
[71] M. Mitrus, Glass Transition Temperature of Thermoplastic Starches, 2005. http://www.international-agrophysics.org/pdf-106643-37485?filename=37485.pdf. (Accessed 14 April 2025).
[72] T. El-Basheer, A. Shehap, K. Mahmoud, M. Abd El-Kader, Preparation and thermal properties of Gelatin/TGS composite films [online] Current Research Web, Middle East Journal of Applied Sciences (2015) 157–170. Available at: https://www.curresweb.com/mejas/mejas/2015/157-170.pdf. (Accessed 14 April 2025).
[73] P. Liu, L. Yu, X. Wang, D. Li, L. Chen, X. Li, Glass transition temperature of starches with different amylose/amylopectin ratios, J. Cereal. Sci. 51 (3) (2010) 388–391, https://doi.org/10.1016/j.jcs.2010.02.007 [online]. (Accessed 14 April 2025).
[74] Sadeghvishakei, M., Yunus, R., Amran, M., Salleh, M. and Pignolet, A. (2011). Mechanical investigation in whiskerized carbon fiber/polypropylene composite. [online] ResearchGate. Available at: https://www.researchgate.net/publication/228448570_MECHANICAL_INVESTIGATION_IN_WHISKERIZED_CARBON_FIBERPOLYPROPYLENE_COMPOSITE [Accessed 6 February. 2025].
[75] K. Yoganandam, V. Shanmugam, A. Vasudevan, D. Vinodh, N. Nagaprasad, B. Stalin, A. Karthick, C. Malla, M. Bharani, Investigation of dynamic, mechanical, and thermal properties of Calotropis procera particle-reinforced PLA biocomposites, Adv. Mater. Sci. Eng. 2021 (1) (2021), https://doi.org/10.1155/2021/2491489 [online].